Journal of Hydroscience and Hydraulic Engineering
Vol. 28, No.1 May, 2010, 87-101

INFLUENCE OF DIFFERENCES IN URBAN STRUCTURE AND ELECTRIC POWER DEMAND ON ATMOSPHERIC THERMAL ENVIRONMENT IN OSAKA URBAN AREA

By

Yukitaka Ohashi

Faculty of Informatics, Okayama University of Science, Kita-ku, Okayama, Japan

Hidemasa Kuroyanagi

Graduate School of Informatics, Okayama University of Science, Kita-ku, Okayama, Japan

Yukihiro Kikegawa

School of Science and Engineering, Meisei University, Hino, Tokyo, Japan

Kazutaka Oka

Mizuho Information & Research Institute, Inc., Chiyoda-ku, Tokyo, Japan

Yoshinori Shigeta

Graduate School of Natural Science and Technology, Okayama University, Kita-ku, Okayama, Japan

Yujiro Hirano

Graduate School of Environmental Studies, Nagoya University, Chikusa-ku, Nagoya, Japan

Hiroyuki Kusaka

Center for Computational Sciences, University of Tsukuba, Tsukuba, Ibaraki, Japan

and

Fei Chen

National Center for Atmospheric Research, Boulder, CO, USA

SYNOPSIS

This paper shows how the micro-scale (1km-square) thermal environment is affected by the building structure and anthropogenic heat, especially, for cooling demands during the summer. Office-building and residential-housing districts in Osaka City were chosen for our observations and numerical experiments. A comparison of results between weekdays and holidays revealed that the waste heat due to air-conditioning operations plays an important role in the rising of air temperature in office-building district, but can be neglected in residential district. From the numerical experiments, the daytime sensible-heat supply in the office-building district was mainly occupied by the waste heat due

to air-conditioning operations; it took about 40 % of all sensible-heat fluxes. On the other hand, the daytime sensible-heat supply in the residential-building district was mainly occupied by the sensible heat from roof surfaces, which accounted for about 30 % of all sensible-heat fluxes.

INTRODUCTION

Heat-island phenomenon (i.e., urban-air temperature becomes higher than that of rural area) is generated due to the sensible-heat supply from artificial surface, the anthropogenic heat, and the urban radiation environment formed by building canyon structures. The introduction of heat-island countermeasures such as the green roofs, high-albedo paints, and water-retentive pavement are recommended by the Ministry of the Environment and local governments. So far, the quantitative effects of the countermeasures on urban thermal environment have been evaluated by means of numerical simulations (1) (2) (3).

The waste heat emitted from exterior unit due to air-conditioning operations also increases the urban-air temperature during the summer. Ohashi et al. (4) suggested that the near-surface air temperature at office buildings in Tokyo metropolitan area increased to about 1℃ due to the waste heat. Narumi et al. (5) indicated that the nighttime waste heat efficiently increased urban-air temperature. The high temperature induces more cooling demands, and then such a cooling will produce much waste heat due to air-conditioning operations. As a result, the vicious spiral is generated between the urban-air temperature and cooling demands. The relationship between the urban thermal environment and cooling electric consumption has been investigated by some researchers for the 23 wards of Tokyo (6) (7). Although such studies provided a validity of waste heat reduction as a heat-island countermeasure, grasping the actual conditions of waste heat in various urban districts is essential for being able to develop the countermeasures effectively. This is because of being strongly concerned with human activities inside buildings for the amount and time evolution of waste heat.

The influence of urban building structure and waste heat on the urban atmosphere possibly varies according to the main type of buildings constructed in each urban district. Therefore, heat-island countermeasures should be suitably introduced for each urban district after making a primary factor of the rising of air temperature clear. Past studies in Japan concerning heat-island issue and its countermeasures have been intended for one specific district with specified building-types in Tokyo metropolitan area. Moreover, few studies have been conducted to examine the influence of cooling waste-heat on urban-district temperature from both numerical simulations and field measurements. This is true not only Japan but also the other countries.

This paper aims at a mechanism forming urban-air temperature from field observations and numerical simulations for the actual urban district in Osaka City described as follows: we (a) investigate the difference in measured temperature among variously utilized urban-districts, (b) consider a relationship between the above temperature differences and the electric power demands, and (c) make a primary factor generating the temperature differences clear through the comparison among some sensible-heat components transported into the urban atmosphere.

NUMERICAL MODEL

In our study, the model coupled with a meso-scale meteorological model (WRF) (8), an urban-canopy atmospheric model (CM) (9), and a building energy consumption model (BEM) (6) was used for reproducing the atmospheric thermal environment in urban districts with a horizontal scale of 1 km. While the WRF predicts the meteorological changes within tens of kilometers to hundreds of kilometers, the CM predicts those with hundreds of meters. The BEM, moreover, calculates the heat loads inside buildings and the waste heat emitted into the urban

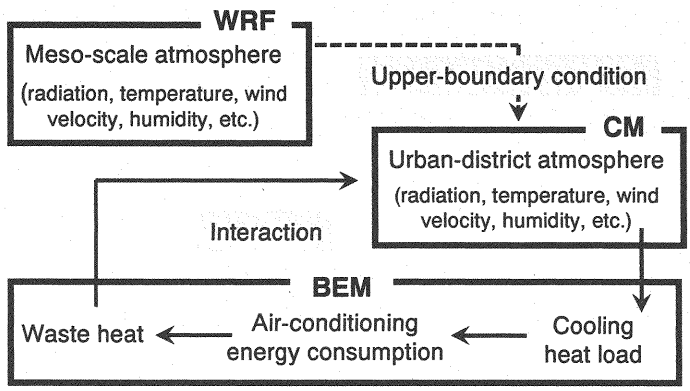

Fig. 1 Calculation flow of the coupled numerical model.

atmosphere due to air-conditioning operations. The calculation flow coupled among the models is shown in Fig. 1.

Meso-scale meteorological model (WRF)

The WRF (Weather Research & Forecasting Model)-ARW Ver.2.2, developed by NCAR (National Center for Atmospheric Research), is a numerical model composed of the fluid-dynamics equations with fully compressible fluid and non-hydrostatic equilibrium. In this model, various physical processes such as land-surface, microphysics, atmospheric boundary-layer are considered.

A calculation domain was chosen to include the whole area of Osaka City. The horizontal grid scales were 1 km, 3 km, and 9 km for the nested three domains. The initial and boundary conditions for the model atmosphere, sea-surface temperature, and soil properties were adopted from meso-scale objective analysis data of the Japan Meteorological Agency and the final analysis data of NCEP (National Center for Environmental Prediction). Other details of the model are described on the WRF web site (8).

Urban-canopy atmospheric model (CM)

The CM, developed by Kondo and Ryu (9), is a multi-layer urban atmospheric model based on vertically one-dimensional diffusion equations. This model assumes the arrangement of same-sized buildings like a perpendicular in shape. The height of buildings averaged in the urban district is considered as the floor density rate at some height, $P_m(z)$. The basic equations of wind velocity (u, v), temperature (potential temperature θ), and humidity (specific humidity q) are given as follows:

$$\frac{\partial u}{\partial t} = \frac{1}{m}\frac{\partial}{\partial z}\left(K_m m \frac{\partial u}{\partial z}\right) - c_d a u\left(\sqrt{u^2+v^2}\right) + fv \tag{1}$$

$$\frac{\partial v}{\partial t} = \frac{1}{m}\frac{\partial}{\partial z}\left(K_m m \frac{\partial v}{\partial z}\right) - c_d a v\left(\sqrt{u^2+v^2}\right) - fu \tag{2}$$

$$c_p\rho\frac{\partial\theta}{\partial t}=c_p\rho\frac{1}{m}\frac{\partial}{\partial z}\left(K_s m\frac{\partial\theta}{\partial z}\right)+Q_{Ws}+Q_{Rs}+Q_{As}+Q_{Vs} \tag{3}$$

$$\iota\rho\frac{\partial q}{\partial t}=\iota\rho\frac{1}{m}\frac{\partial}{\partial z}\left(K_l m\frac{\partial q}{\partial z}\right)+Q_{Wl}+Q_{Rl}+Q_{Al}+Q_{Vl} \tag{4}$$

where, m = effective volume ratio of urban canopy air:

$$m=1-\frac{b^2}{(w+b)^2}P_w(z) \tag{5}$$

The symbol w and b represent the road width and building width averaged in the district, respectively. The building's surface area density per unit volume, a, is calculated by

$$a=\frac{bP_w(z)}{(w+b)^2-b^2P_w(z)} \tag{6}$$

Q_{Ws}, Q_{Rs}, Q_{As}, and Q_{Vs} in Eq. 3 represent the sensible-heat transports (fluxes) from the building roofs, side-walls, the air-conditioning exterior unit, and by ventilation, respectively. Similarly, Q_l in Eq. 4 means the above latent-heat components. The other symbols in these equations are listed in the Appendix.

Calculations of the sensible- and latent-heat transported from each building surface need to solve the surface heat budget equation. Thus, the radiation flux at each model layer is calculated by considering the sky view factor and building shade, which assumes that the building walls face due north, south, east, and west. The area of building shades is geometrically calculated from the relationships between the solar azimuth and altitude, and the building height and distance. Other details of the model are described by Kondo and Ryu (9). The various parameters set up within CM are summarized in Table 1. The building widths b averaged in the office-building and the residential-housing districts were 16.5 m and 10.5 m, respectively, which were estimated from the building polygon data of Osaka City. On the other hand, the road widths w averaged in the office-building and the residential-housing were 6.7 m and 6.0 m, respectively. The vertical building distributions, $P_w(z)$, in the office-building and residential-housing are also shown in Fig. 2.

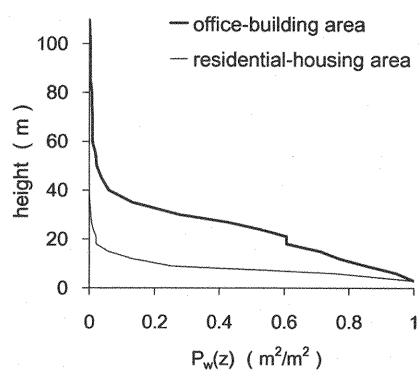

Fig. 2 The vertical building distributions, $P_w(z)$, in the office-building and the residential-housing.

Table 1 Parameters used in CM.

		Office-building area	Residential-housing area
Building bodies			
Albedo		0.19	0.19
Emissivity		0.96	0.96
Volumetric heat capacity	roof	1.60×10^6 J/m^3 · K	0.93×10^6 J/m^3 · K
	heat insulator	0.05×10^6 J/m^3 · K	none
	side wall	1.79×10^6 J/m^3 · K	0.89×10^6 J/m^3 · K
Thermal conductivity	roof	0.47 W/K · m	0.22 W/K · m
	heat insulator	0.03 W/K · m	none
	Side wall	0.67 W/K · m	0.30 W/K · m
Windows			
Sunlight transmissivity		30.0 %	50.0 %
Area ratio		33.1 %	18.0 %
Roads			
Albedo		0.19	0.19
Emissivity		0.96	0.96
Volumetric heat capacity	upper	1.92×10^6 J/m^3 · K	1.90×10^6 J/m^3 · K
	lower	1.74×10^6 J/m^3 · K	1.74×10^6 J/m^3 · K
Thermal conductivity	upper	1.37 W/K · m	0.70 W/K · m
	lower	1.00 W/K · m	1.00 W/K · m
Vegetation ratio		3.4 %	20.0 %

Building energy consumption model (BEM)

The BEM, developed by Kikegawa et al. (6), is a numerical model which predicts the heat exchange process between the urban atmosphere and building inside. In this model, the interior heat-budget is calculated for the building like a one box model. The heat loads within room (H_{in} and E_{in}) are mainly divided into the solar permeation through the window, the conductive heat through the walls, the heat inflow due to ventilation, illuminants and office automation appliances, and the generated heat of the human body.

$$H_{in} = \sum_i A_i h_i \left(W_i - T_r\right) + \sum_j A_j \eta_j S_j + (1-\beta) c_p \rho V_a \left(T - T_r\right) + A_f Q_{el} + A_f P \phi_p Q_{hs} \qquad (7)$$

$$E_{in} = (1-\beta)\iota\rho V_a (q - q_r) + A_f P \varphi_p Q_{hl} \tag{8}$$

where, W (K) = the indoor wall-surface temperature; T (K) = the outdoor-air temperature; S (W/m^2) = the solar irradiance through the window; β (−) = the thermal efficiency of the total heat exchanger; V_a (m^3/s) = the volume of the outdoor-air inflow. The subscripts i and j represent the surface elements of the indoor wall and the window, respectively. The symbols A_i (m^2) and A_j (m^2) are their areas. The first term on the right of Eq. (7) is the heat conduction on the building roof and wall. The second term is the solar insolation through the window. The third term denotes the sensible heat loads by ventilation. The fourth and the last terms are the sensible heat generations from equipment and workers in the building, respectively. Here, Q_{el} (W/m^2) the amount of sensible heat generated from equipment, and Q_{hs} (W/person) the amount of sensible heat generated from workers.

On the other hand, Eq. (8) is the latent heat component of the thermal heat loads indoors, which consists of the latent heat loads by ventilation (the first term) and the indoor latent-heat generated from the workers (the second term). The symbol Q_{hl} (W/person) is the amount of latent heat generated from workers. The other symbols in these equations are listed in the Appendix.

These heat loads are pumped out to the urban atmosphere by the air-conditioning operation (Q_A in Eqs. 3 and 4). The heat-budget process between the outside atmosphere and building inside determines the room temperature (T_r) and humidity (q_r) as follows:

$$Q_B \frac{dT_r}{\partial t} = H_{in} - H_{out} \tag{9}$$

$$\iota\rho V_B \frac{dq_r}{\partial t} = E_{in} - E_{out} \tag{10}$$

The symbols H_{out} and E_{out} are the sensible and latent heat pumped out from the building for cooling, respectively:

$$H_{out} = \zeta\gamma\left(H_{in} + Q_B \frac{T_r - T_{set}}{\Delta t}\right) \tag{11}$$

$$E_{out} = \zeta\gamma\left(E_{in} + \iota\rho V_B \frac{q_r - q_{set}}{\Delta t}\right) \tag{12}$$

The symbols T_{set} (K) and q_{set} (kg/kg) are the target temperature and specific humidity of the room cooling by air-conditioner. The waste heat from exterior unit consists of the sum of the energy (electricity or town gas) consumed by the air-conditioner and the interior heat removed by the air-conditioning operation:

$$Q_A = EC + (H_{out} + E_{out}) \tag{13}$$

The air-conditioning energy consumption (EC) that is required to estimate Q_A is given by

$$EC = \frac{H_{out} + E_{out}}{COP} \tag{14}$$

where, *COP* = the coefficient of performance of the heat pump system. The *COP* represents the overall energy efficiency of the air-conditioner. Its magnitude depends on each type of air-conditioning system. The other symbols in the equations are listed in the Appendix.

The various parameters set up in BEM are summarized in Tables 2 and 3. Other details of the model are described by Kikegawa et al. (6). Ohashi et al. (4) verified sensitivities of the parameters in CM and BEM. Their findings revealed that the change of surface-air temperature was less than 0.1 ℃ if any parameters varied with valid range.

Table 2 Parameters used in BEM.

	Office-building area	Residential-housing area
Air-conditioning times	7:00－23:00 JST	1:00－24:00 JST
Target temperature of room cooling	26.0 ℃	26.0 ℃
Target humidity of room cooling	50.0 %	50.0 %
Ratio of air-conditioning types (air-cooled : water-cooled)	7 : 3	10 : 0
Ratio of possible air-conditioned floor area to total floor area	60 %	40 %
Volumetric ventilation rate per unit floor area	4.0 $m^3/m^2 \cdot h$	1.0 $m^3/m^2 \cdot h$
Persons per floor area	0.13 person/m^2	0.02 person/m^2
Heat generation from person	sensible-heat: 54.7 W/m^2 latent-heat: 64.0 W/m^2	sensible-heat: 54.7 W/m^2 latent-heat: 64.0 W/m^2
Location of ventilating opening	every floor	every floor

Table 3 Parameters used in BEM (continued).

	Air-conditioning type	Cooling type	Energy	COP	Waste heat emission	Occupied rate
Office-building area	directly-fired absorption chiller-heater	water-cooled	town gas	0.97	roof	32.1 %
	turbo chiller	water-cooled	electricity	4.71	roof	18.9 %
	building-multi heat pump	air-cooled	electricity	2.58	roof	24.5 %
					ground	24.5 %
Residential-housing area	heat pump	air-cooled	electricity	4.50	every floor	100.0 %

OBSERVATIONS

Outline

Our meteorological observations were conducted during the period of August 1-14, 2007, when the Pacific high-pressure covered with Japan. The office-building district is located in Chuo-ward in Osaka City, while the residential-housing district is located in Higashisumiyoshi-ward. Many observation sites (fixed-ten sites within 1 km-square) were provided for the heterogeneous temperature distribution due to locality of anthropogenic heat, radiation, and turbulence. The surface-air temperatures were measured at height of about 2 m over the edge of north-south, west-east, and cross roads. We adopted the average value of the ten-site temperatures as a representative temperature of the urban district. Observation maps of site locations are shown in Fig. 3.

In our observations, portable temperature measurements with thermistor sensor (RTR-52; T&D Co.) were used by covering with a radiation shield. The interval of data sampling was 30 seconds, and these data were averaged between 10 minutes for analysis.

Furthermore, the data of electric power demands were provided by Kansai Electric Power Co., Inc., which were measured in two areas including the districts in our study during the period of meteorological observations. A major building type in the areas where the electric power data were measured is almost consistent with that in the districts examined: office-buildings and residential-housings.

Measured temperatures

Figure 4 shows the temporal variations of surface-air temperature measured in the office-building district, the residential-housing district, and Osaka Meteorological Observatory (located beside the office-building district). This figure represents the temperature for 9 days except August 1-3 (influence of typhoon) and August 13-14 (Japanese special holidays). We compared the air temperature of our measurement with that of Osaka Meteorological Observatory by setting up very near the temperature measurement of Osaka Meteorological Observatory for a few days. As a result, there was a difference of 0.2℃ at the maximum between these measurements. In this figure, it was revealed that the daytime temperature in the residential-housing district was higher than that in the office-building

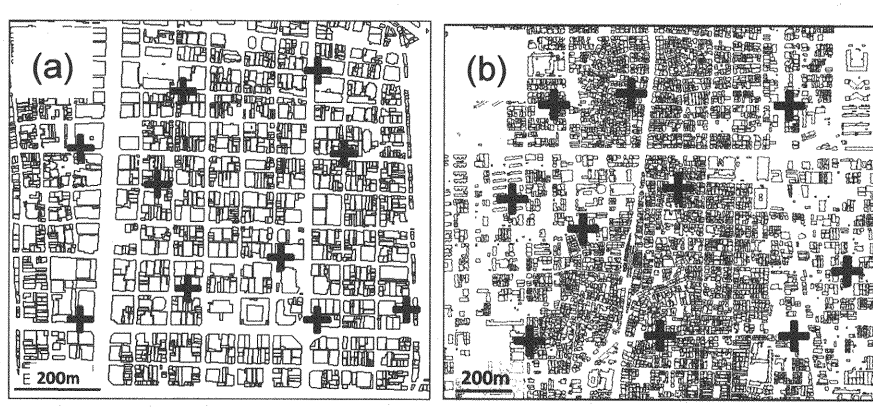

Fig. 3 Maps of observation sites (cross symbols) in (a) office-building and (b) residential-housing districts.

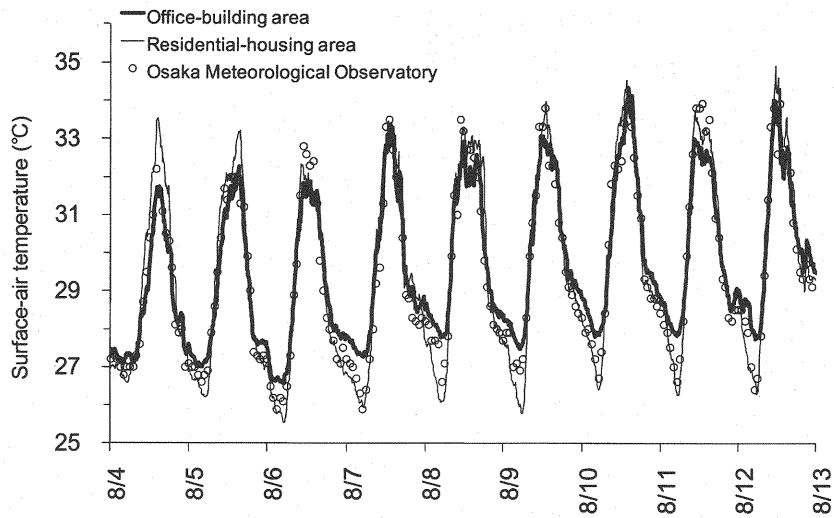

Fig. 4 Temporal variations of the averaged surface-air temperatures in office-building and residential-housing districts during the observation period (August 4-12, 2007). Also, surface-air temperature measured at Osaka Meteorological Observatory is shown.

district almost every day (a maximum of 2.0℃ at 1430 JST of August 4), whereas the nighttime temperature at the office-building district became higher than that at the residential-housing district every day (a maximum of 1.8℃ at 0400 JST of August 8).

Although Osaka Meteorological Observatory is located near the office-building district, the temperatures measured at there were during daytime higher than those in the office-building district and during nighttime lower than in that. Therefore, the time variation of temperature measured by Osaka Meteorological Observatory was similar to that of residential-housing district rather than office-building district. This finding suggests that the measurements of the multi-site temperatures within actual urban-district are required to grasp an urban thermal environment with a district scale.

NUMERICAL SIMULATIONS

Electric power demands

The electric power demands (per total floor-area) measured actually by a substation and calculated by our numerical model are indicated in Fig. 5. Weekdays and holidays correspond to 5 days of August 6-10 and 4 days of August 4-5, 11-12, respectively. For the electric power measured in the office-buildings, the daytime demands reached 2.7 times in average as much as the holiday those. On the other hand, the electric power in the residential-housings barely changed between weekdays and holidays. Whereas the time variations of electric power demands simulated in the office-building district were very consistent with those measured, the daytime electric power demands simulated in residential-housing district were about twice overestimated in comparison with the measured peak demands. An analysis of the results of our calculation revealed that about 64 % difference in electric power demands between weekday and holiday was attributed to air-conditioning operations.

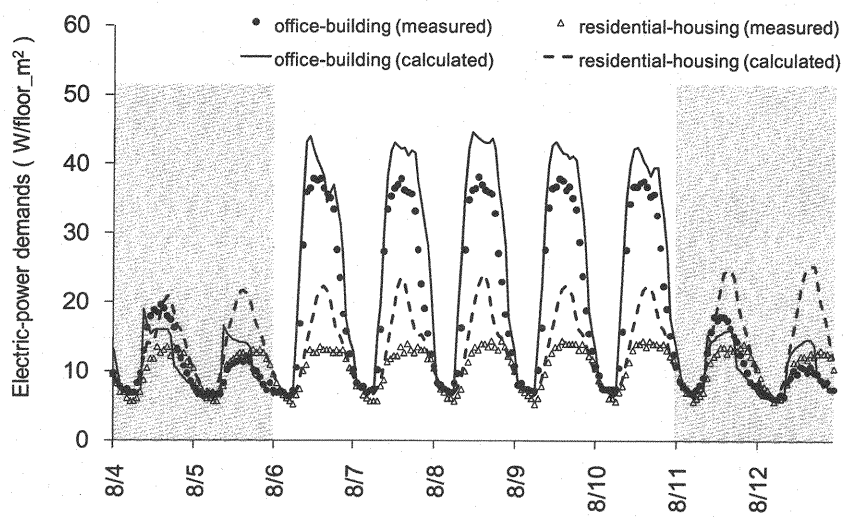

Fig. 5 Temporal variations of the electric power demands measured and calculated during the observation period (August 4-12, 2007). Shaded days (August 4, 5, 11, and 12) mean holidays (Saturday and Sunday).

Urban-district temperature

Figure 6 shows the temperature differences between the office-building and residential-housing districts during the observation period. These differences indicate the office-building temperature minus the residential-housing temperature. The model surface-air temperature is calculated at a height of 3 m of the model lowest layer. August 4, 5, 11, and 12 correspond to holidays during the period. The daytime temperature calculated in the residential-housing district was higher than that in the office-building district, which was the same feature as the measured. In addition, both temperature differences on holidays between the both districts tend to be more extended than those on weekdays, excluding a few exceptions. On the other hand, the nighttime temperatures difference calculated by the model were not reproduced well; the temperatures in the both districts were little difference between each other.

Here, we quantitatively evaluate the influence of the electric power change on the difference of urban-district temperatures, from the fact of that the office-building electric power demands greatly varied between weekday and holyday. The daily surface heat budget is thought to be not greatly different among each other because the clear and calm days continued stably during our analysis period. Therefore, if the temperature difference between the office-building and residential-housing districts was not the same systematically on weekdays and holidays, this is possibly attributed to reflecting influence of the air-conditioning waste heat. The change in difference between weekdays and holidays reached to a maximum of 1℃, which was due to change of about 25 W/m^2 per the total floor area on average, from comparison of the electric power demands measured between weekdays and holidays of Fig. 5; this change is due to the increase and decrease of the air-conditioning waste heat. Also, the result of calculation provided that the absolute temperature difference on weekday differed from that on holiday to a maximum of 0.8℃. This feature was induced by decrease in the air-conditioning electric power demands of 30 W/m^2 in the office-building district from Fig. 5.

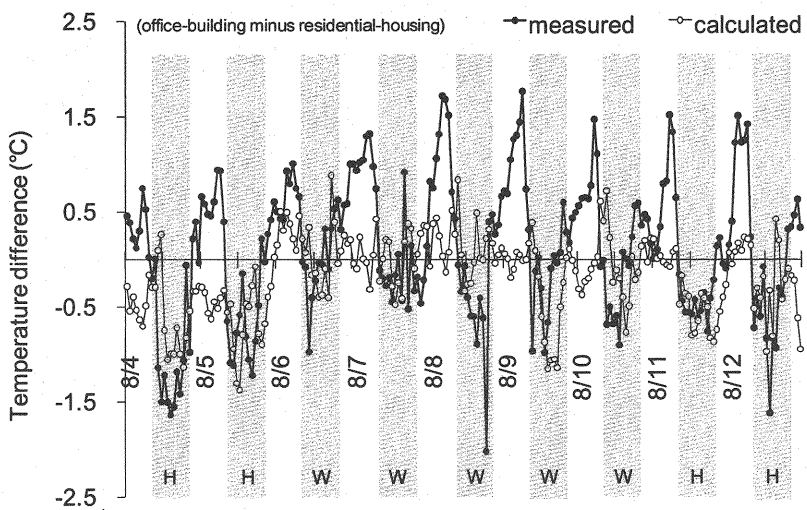

Fig. 6 Temporal variations of the temperature differences between the office-building and residential-housing districts during the observation period (August 4-12, 2007). These differences show the office-building temperature minus the residential-housing temperature. The shaded areas mean daytime hours (8-20 JST). "H" and "W" represent the daytimes of holidays and weekdays, respectively.

ANALYSIS OF URBAN-DISTRICT HEAT BUDGET

Here, we investigated which of sensible-heat components greatly affected the urban-district temperature through comparison among the sensible-heat transports (of the terms on the right hand of Eq. 3) from building roofs, side-wall, road, air-conditioning exterior unit, and by ventilation. The result of heat budget at the lowest layer (3 m in height) is shown in Figs. 7 and 8. As can be seen in Figs. 7a and 7a, especially, the sensible-heat supplies from road surface in the office-building district were smaller than those in the residential-housing district; its maximum difference is about 120 W/m^2. At 1200 JST when the solar altitude is at its highest point, the ratio of the shaded area to the whole road area was 100 % in the office-building district and 40 % in the residential-housing district, respectively. Those shading-ratio values were geometrically and simply estimated from the model building-height and road-width. This finding suggests that it is difficult to insolate the road surface in the office-building district with tall buildings.

In the office-building district (Fig. 7), a total sensible-heat transport into the atmosphere on weekday was greater than that on holiday at the maximum of 180 W/m^2 (unit land area); its magnitude was almost consistent with the increase of air-conditioning waste heat. In addition, the weekday waste-heat amount from 06 JST to 00 JST when people are active within buildings accounted for more than 40 % of the total sensible-heat flux. Hence, this result shows that the influence of waste heat on the urban thermal environment should not be neglected in a district where people are active. Also, the sensible-heat supply from office-building roofs on weekday occupied 35% (143 W/m^2) of the total amount at the maximum. On the other hand, the sensible-heat supply from the building side-wall was considerably small during daytime, and then at nighttime its ratio to the total sensible-heat flux became larger up to more than 20 % in spite of a small magnitude. The sensible-heat flux at the road surface was also small like a building roof. From these results, we concluded that the heat-island countermeasures introduced into building roofs and air-conditioning waste heat are effective to control the urban-air temperature in office-building district of Osaka City.

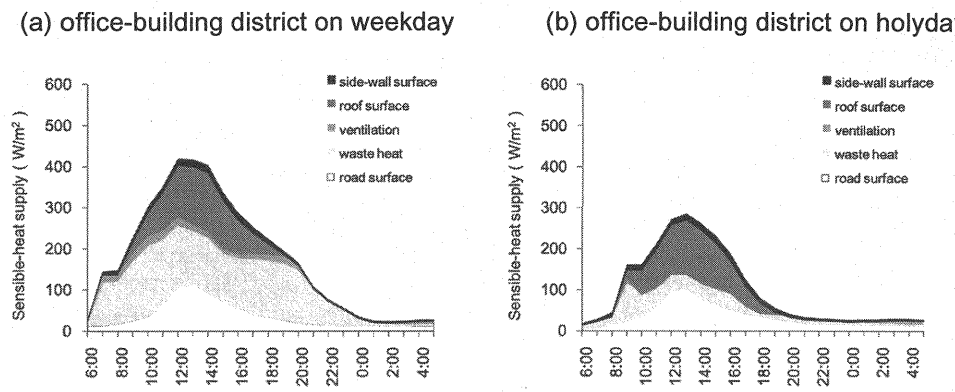

Fig. 7 Temporal variations of the amount of sensible-heat supply in office-building district. The ensemble mean values at the lowest layer are shown for (a) weekday and (b) holiday based on unit land area.

In the residential-housing district (Fig. 8), the sensible-heat flux did not almost change between weekdays and holidays because of unchanged waste heat amount relative to the other sensible-heat components. The sensible-heat transport from the roof surface occupied during daytime, especially 30 % of the total amount at the maximum. We consider that the sensible-heat supply from lower roof surfaces affects the air temperature nearby surface. On the other hand, the sensible-heat supply from the road surface in the residential-housing district became greater than that in the office-building district previously mentioned. The sensible-heat flux from the road primarily occupied more than 40% of the total flux during the daytime; it is related to the small shaded area on the road surface in the residential-housing district, as mentioned before. From these results, we concluded that the heat-island countermeasures introduced into roof and road surfaces are effective in controlling the urban-air temperature in residential-housing districts of Osaka City.

CONCLUSION

In this study, the urban thermal environment and electric power demands were analyzed to quantitatively clarify the influence of difference in urban-district (building) types and human activities on the urban surface-air temperature. Findings of this study are summarized as follows:

(a) The nighttime-air temperature measured in the Osaka office-building district was 1.8 ℃ at the maximum higher than that in the Osaka residential-housing district, whereas the daytime temperature in the office-building district was 2.0 ℃ at the maximum lower than that in the residential-housing district, during our observations. Also, the air temperatures measured at the Osaka Meteorological Observatory, which was located within the same type of urban-district as our office-building district, were separated from the office-building temperatures actually measured; it suggested that the measurements of the multi-site temperatures within actual urban-district are required to grasp an urban thermal environment with a district scale.

(b) Our comparison in urban-district temperature between weekdays and holidays revealed the influence of air-conditioning waste heat on the surface-air temperature; the change of electric power demands in office-building district of 25 W/m^2 per the total floor area induced a change of 1 ℃ for surface-air temperature of urban-district. A similar sensitivity also appeared in the model calculations.

(a) residential-housing district on weekday (b) residential-housing district on holyday

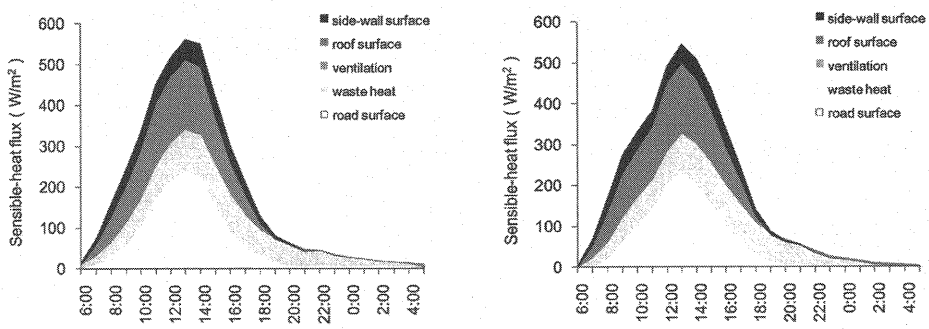

Fig.8 Same as Fig. 7 but for residential-housing district.

(c) With a numerical model including an urban-district structure and building energy consumption, the thermal environment in each urban-district was analyzed. Numerical simulations were able to reproduce a difference of temperatures and electric power demands obtained from observations between weekdays and holidays. It was confirmed that air-conditioning waste heat was important for heating mechanism of the urban atmosphere; this means that there is a strong interaction between the urban atmosphere and human activity inside buildings.

(d) Heat-island countermeasures should be suitably introduced by taking a difference of urban-district structures and human activities into consideration. From our heat-budget analysis with a numerical model, we determined that heat-island countermeasures should be introduced for roof surfaces and waste heat in daytime office-building district, while for road and roof surfaces in daytime residential-housing district in Osaka City.

ACKNOWLEDGEMENTS

The data of electric power demands were provided by the Kansai Electric Power Co., Inc. The establishment of our meteorological instruments was supported by Osaka City and the Kansai Electric Power Co., Inc. The building polygon data of Osaka City was provided by Osaka City.

REFERENCES

1. Taha H., Akbari H., Rosenfeld A., and Huang J. : Residential cooling loads and the urban heat island－The effects of albedo, Building and Environment, Vol.23, No.4, pp.271-283, 1988.
2. Sato T., Murakami S., Ooka R., Yoshida S., Harayama K., and Kondo H. : Numerical study on effects of countermeasures for urban heat island in summer and winter－The characteristic of urban climate and effects greening and high albedo surface－, Journal of Environmental Engineering, No.577, Architectural Institute of Japan, pp.55-62, 2004 (in Japanese).
3. Kondo H., Kikegawa H., Genchi Y., Ihara T., Ohashi Y., and Tokairin T. : Assessment of countermeasures against heat island with a combined model of urban climate, urban canopy and building energy consumption, Journal of Heat Island Institute International, Vol.1, Heat Island Institute International, pp.53-57, 2006 (in Japanese).

4. Ohashi, Y., Genchi, Y., Kikegawa, Y., Kondo, H., Yoshikado, H., and Hirano, Y. : Influence of air-conditioning waste heat on air temperature in Tokyo office areas during summer: Numerical experiments using an urban canopy model coupled with a building energy model, Journal of Applied Meteorology and Climatology, Vol.46, No.1, American Meteorological Society, pp.66-81, 2007.
5. Narumi D., Otani F., Kondo A., Shimoda Y., and Mizuno M. : Effect of anthropogenic waste heat upon urban thermal environment－Analyses of countermeasures for mitigating heat islands phenomena using a numerical model Part 1－, Journal of Architecture, Planning and Environmental Engineering, No.562, Architectural Institute of Japan, pp.97-104, 2002 (in Japanese).
6. Kikegawa Y., Genchi Y., Yoshikado H., and Kondo H. : Development of a numerical simulation system toward comprehensive assessments of urban warming countermeasures including their impacts upon the urban buildings' energy demands, Energy and Resources, Vol.22, No.3, Japanese Society of Energy and Resources, pp.235-240, 2001 (in Japanese).
7. Harada Y., Murakami S., Ooka R., Harayama K., Sato T., and Kawamoto Y. : Urban climate analysis based on local climate model coupled with heat release model through air conditioning, Journal of Environmental Engineering, No.597, Architectural Institute of Japan, pp.65-71, 2005 (in Japanese).
8. Weather Research & Forecasting Model : http://wrf-model.org/index.php
9. Kondo H. and Liu F.-H. : A study on the urban thermal environment obtained through one-dimensional urban canopy model, Journal of Japan Society for Atmospheric Environment, Vol.33, No.3, Japan Society for Atmospheric Environment, pp.179-192, 1998 (in Japanese).

APPENDIX – NOTATION

The following symbols are used in this paper:

a = building surface area per unit volume (m^2/m^3);

A_f = the floor area of the building (m^2) ;

c_d = drag coefficient due to buildings;

c_p = specific heat at constant pressure (J/kg・K);

f = Coriolis parameter (/s);

h = the convective heat transfer coefficient (W/m^2・K);

K_l = vertical diffusivity for water vapor (m^2/s);

K_m = vertical diffusivity for momentum (m^2/s);

K_s = vertical diffusivity for heat (m^2/s);

m = the effective volume ratio of canopy air (m^3/m^3);

P = the maximum number of the workers per floor area (person/m^2);

q = specific humidity (kg/kg);

Q_B = the overall heat capacity of the room air (J/K);

Δt = time step for the model integration (s);

u = wind speed of west-east component (m/s);

v = wind speed of south-north component (m/s);

V_B = the total volume of the room air (m^3);

γ = the ratio of possible air-conditioned floor area to the overall floor area within a building ($0 \leqq \gamma \leqq 1$);

ζ = the ratio of actual air-conditioned floor area at some hour to the maximum possible air-conditioned floor area ($0 \leqq \zeta \leqq 1$);

η = the sunlight transmissivity of the window ($-$)

θ = potential temperature (K);

ι = the latent heat due to the evaporation (J/kg);

ρ = air density (kg/m^3); and

φ_p = the ratio of hourly working persons number to P ($0 \leqq \varphi_p \leqq 1$).

(Received Aug 01, 2009 ; revised Feb 15, 2010)